Alam Cipta Int. J. Sustain. Trop. Des. Res. Pract. 19 (2): 175-202 (2026)

ALAM CIPTA

Sustainable Tropical Design Research and Practice

Journal Homepage: http://alamcipta.upm.edu.my/

Quantitative Reference for "Constant-Holistic Shadow" Space in North–South Campus Buildings of Hot-Summer Regions: A Study Based on the Averaged Sky View Factor

Luo Guohui[1, 2], Nik Lukman Nik Ibrahim[1, *], Wang Zhiyun[1, 2], Li Jinyan[1], Wang Yunxuan[1], Cui Kaiyi[2], Gong Ziping[2], Huang Lijun[2], Huang Huaqing[2] and Luo Wenjing[3]

[1]*Faculty of Engineering and Built Environment, Universiti Kebangsaan Malaysia, 43600, Selangor, Malaysia*
[2]*Faculty of Urban Construction, Guangzhou Huali College, 511300, Guangzhou, China*
[3]*Faculty of Arts and Social Sciences, Universiti Malaya, 50603, Kuala Lumpur, Malaysia*

ABSTRACT

The midday period from 12:00 to 14:00 is a critical exposure window on university campuses, during which teachers and students frequently move outdoors for class transitions and meals. Effectively constructed "Constant-Holistic Shadow" (CHS) spaces can provide continuous and accessible shade, allowing users to carry out outdoor activities without passively seeking shelter from the sun. This study examined the space-time in need of shadow for university teachers and students in Guangzhou. The area-averaged Sky View Factor (SVFa) at 1.5 m was calculated across 210 campus models, and its relationship with the ratio of CHS space area to activity space area (C/A) was analysed. The findings show that: (1) C/A increases significantly when SVFa decreases from approximately 0.35 towards 0 across the tested dates; (2) when SVFa ≤ 0.111, CHS space with C/A ≥ 60% can be achieved for all tested dates; and (3) building-only layouts provide only 5–20% effective shade between 12:00 and 14:00 from May 24 to September 1. These findings provide a quantitative reference for campus planning, design, and renovation in Guangzhou and other regions at similar latitudes.

Keywords: "Constant-holistic Shadow" Space; area-averaged Sky View Factor; outdoor activities; built Environment

ARTICLE INFO

Article history:
Received: 01 February 2026
Accepted: 28 April 2026
Published: September 2026

DOI: https://doi.org/10.47836/AC.19.2.PAPER09

Email addresses:
P131069@siswa.ukm.edu.my (Luo Guohui)
lukman@ukm.edu.my (Nik Lukman Nik Ibrahim)
wangzhiyun1995@163.com (Wang Zhiyun)
lijinyan789@163.com (Li Jinyan)
P124253@siswa.ukm.edu.my (Wang Yunxuan)
1658664490@qq.com (Cui Kaiyi)
2646126828@qq.com (Gong Ziping)
1559506553@qq.com (Huang Lijun)
976347627@qq.com (Huang Huaqing)
1686822544@qq.com (Luo Wenjing)
* Corresponding author

INTRODUCTION

One of the determinants of the quality of urban life and socio-cultural lifestyle is the thermal comfort of outdoor public spaces (Bajsanski et al., 2016). During the hot and sunny days of summer, insolation profoundly affects the thermal comfort of outdoor activists (Nikolopoulou & Steemers, 2003; W. Yang et al., 2013; Zhou et al., 2016). Without shadow, these individuals often endure constant sun exposure, leading to significantly restricted normal activities in outdoor spaces (Nikolopoulou et al., 2001; Y. Yang et al., 2018). In this context, shade should be understood not only as a passive environmental condition, but also as an essential spatial resource for sustaining outdoor activities under hot-summer conditions.

The shadows of buildings, structures, or plants can effectively mitigate the adverse effects of persistent insolation in hot summers (Peng et al., 2021; Wong & Yu, 2005), by reducing direct solar radiation (Gong et al., 2018; Hsieh et al., 2016; Peng et al., 2017; Saneinejad et al., 2014), decreasing outdoor thermal discomfort (Emmanuel et al., 2007). In urban environments, especially on university campuses, the motivation of teachers and students to engage in outdoor activities relies heavily on the thermal comfort of the public activity spaces (Huang et al., 2019). Good outdoor thermal comfort can encourage teachers and students to engage in social (R. M. A. Mahmoud & Abdallah, 2022) and physical activities (Niu et al., 2020). However, the planning and design of many colleges and universities have not yet been able to fully utilize the shadows of buildings, structures, and plants on campus to mitigate the adverse effects of constant sun exposure, resulting in 40% of the campus shadow being ineffective (Ghaffarianhoseini et al., 2019). Previous thermal-comfort studies in educational environments have tended to focus on indoor settings, such as classrooms, offices, and dormitories, while outdoor light and thermal comfort on university campuses have received comparatively less attention (Lau et al., 2019; Shih et al., 2017). Effectively utilizing shadows to create comfortable outdoor activity spaces remains a crucial topic for university planners, designers, and researchers (Huang et al., 2019; Morakinyo et al., 2016; Taleghani, 2018).

With the increasing refinement of the built environment in China, the combination and arrangement of buildings, structures, and plants facilitate the creation of shadows to address outdoor thermal comfort issues (Lin et al., 2010). CHS space is a natural phenomenon that exists in the outdoor environment under sunlight conditions. It is formed by buildings, structures and plants and other sunlight-blockers independently or in combination, creating shadow areas on the shadow-accepted plane, such as ground. These shadows are limited by the activity time in three-dimensional space, giving them significant spatio-temporal dynamics (Gong Zhaoxian et al., 2021) (Figure 1). In the absence of effective construction, CHS space is often limited in spatial scale. Its shadow periods and locations, as well as the size of the shaded area, do not always align with the space-time needs of outdoor activists exactly.

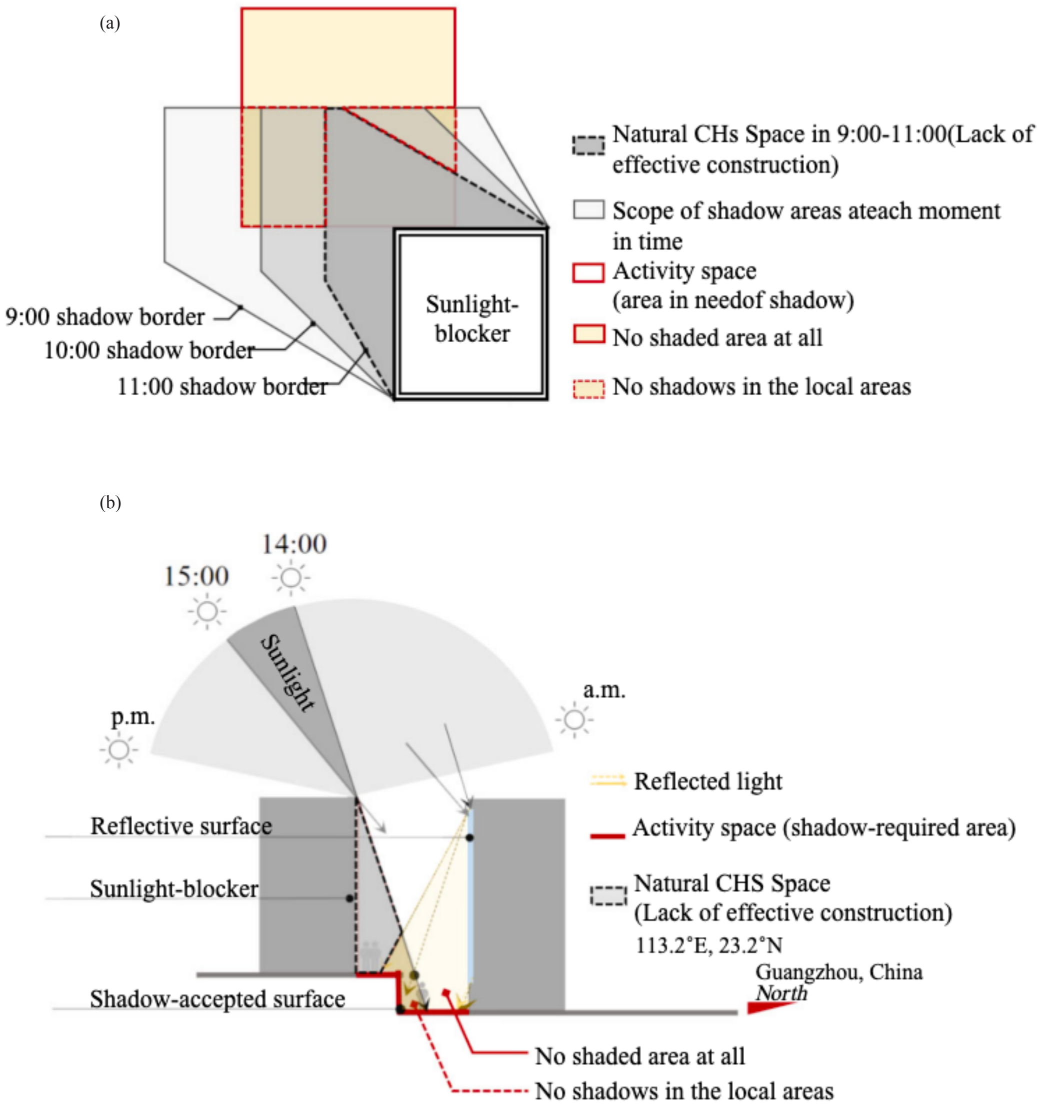

Figure 1. Schematic plan and section of CHS space without effective construction. (a) Plan diagrammatic sketch of CHS space; (b) section diagrammatic sketch of CHS space

Currently, theoretical research on CHS space has mainly focused on three objectives:

i. To discuss the physical properties of sunlight-blockers, such as orientation (Jamei et al., 2016; Peng et al., 2021), external morphology of CHS space (Jamei et al., 2016; Palme et al., 2020; Luo et al., 2025), height-to-width ratio (H. Mahmoud & Ragab, 2020; R. M. A. Mahmoud & Abdallah, 2022), and the distance between sunlight-blockers (Palme et al., 2020).

ii. To explore the formation mechanism of CHS space, investigating the reasons for excessively small CHS space areas, and establishing the mechanisms and design strategies to increase the shadow coverage (Luo Guohui et al., 2021).

iii. To Propose methods for constructing CHS space for different building types, such as creative industrial parks (Cheng Yao, 2020), medical buildings (Lu Xueyao, 2020), and large-scale tourist areas (Fang Yuechao, 2021). Most related studies have examined the formation mechanism of CHS space and proposed generalized design strategies based on building-shadow simulations. However, these previous methods are mainly qualitative or typological, and are more applicable to relatively simple built environments with limited combinations of buildings, structures, and vegetation. They also tend to overlook the complexity of shadow demand caused by geographic conditions, user groups, and activity schedules. As a result, there remains a lack of design-oriented quantitative reference indices that can link built-environment openness with effective CHS-space coverage under specific space-time needs.

Unlike related studies, this research focuses on the specific needs of teachers and students at a university in Guangzhou City, China. It considers the date period, time period, and area in need of shadow. The study simulates and calculates the area-averaged sky view factor (Lin et al., 2012) for 210 different architectural environments. It then quantitatively analyzes the correlation between SVFa and the ratio of the CHS space area to the activity space area to obtain a quantitative index for constructing CHS space. This index can serve as a direct reference for campus design and renovation in Guangzhou and, subject to local climatic calibration, in other hot-summer regions at similar latitudes.

LITERATURE REVIEW

Sky View Factor and Its Relevance to Outdoor Thermal Environment

The geometric characteristics of the built environment have a significant influence on outdoor thermal conditions (G. Chen et al., 2021). These characteristics are commonly described using two indicators: the building height-to-street-width ratio and the SVF (Arnfield, 2003; Unger, 2009; Miao et al., 2020). Compared to the former, SVF provides a more comprehensive description of complex built environments (Johnson & Watson, 1984; Miao et al., 2020), because it determines the solar duration in street canyons (Du et al., 2020). The concept of SVF was first introduced by Oke in 1981 (Oke, 1981) and is defined as the ratio between the radiation received (or emitted) from the sky by a plane and the radiation emitted (or received) by the entire unit hemispheric radiation environment (Watson & Johnson, 1987). In short, it is the ratio of the visible area of the sky within a street canyon, with values ranging from 0 to 1 (Oke, 1981; He et al., 2015), where 0 indicates complete blockage from seeing the sky, and 1 indicates a completely open view of the sky..

SVF can be utilized to assess the heat island effect in urban and built environments (Oke, 1981), predict human thermal perception (Lam et al., 2023), and has been widely applied in areas such as outdoor thermal environments (L. Chen et al., 2012; Chiang et al., 2023), urban planning practices (Bourbia & Boucheriba, 2010; Wei et al., 2016) and surface heat balance (Miao et al., 2020). Therefore, with growing emphasis on improving urban environmental quality under global warming, the effective use of SVF to improve outdoor thermal comfort and enhance built-environment quality has become an important issue in urban climate research and building design.

Methods for Obtaining Sky View Factor

Current SVF estimation approaches can be broadly classified into five main categories (Kim & Yi, 2019; Miao et al., 2020): geometric methods (Johnson & Watson, 1984; Watson & Johnson, 1987), fisheye photographic methods (Matzarakis & Matuschek, 2011), GPS methods (Chapman et al., 2002), street-view-image-based methods (X. Li et al., 2018; Gong et al., 2019) and 3D city-model simulation methods (X. Li et al., 2018; Cheung et al., 2016).

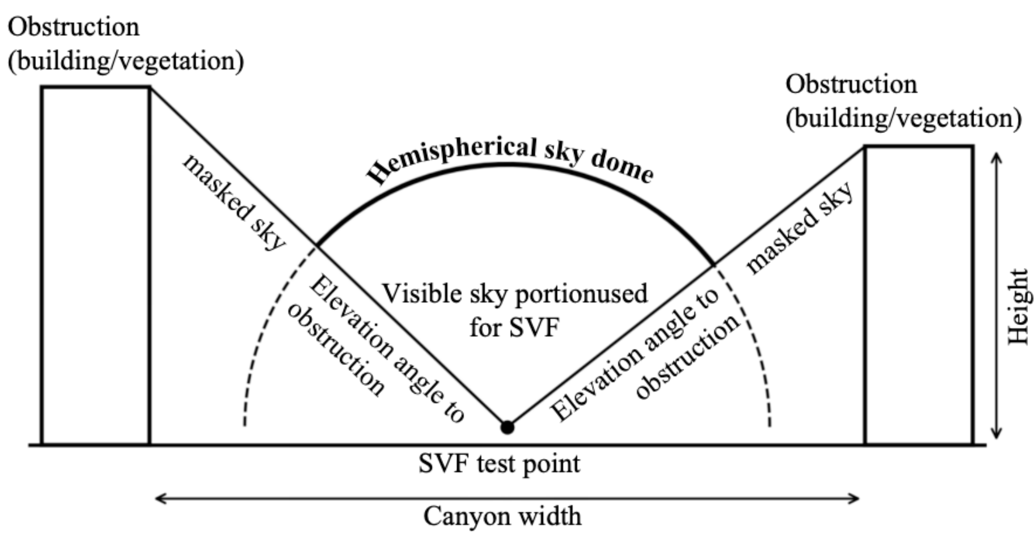

Figure 2. Simplified geometric interpretation of SVF in a street-canyon setting

(1) The geometric method is to calculate the angle from the plane of the environment to the tops of the surrounding buildings, structures and plants within a defined part of the real environment by substituting the formula given by Oke (1981). This type offers more detailed geometric calculations compared to other methods for obtaining SVFs, but it is time-consuming and has limited applicability. Although Johnson and Watson optimized it for asymmetrical canyons of limited length (Johnson & Watson, 1984), it remains less convenient than other methods. These methods are still most applicable to simple and regular built environments (Miao et al., 2020) (Figure 2).), it remains less convenient than other methods. These methods are still most applicable to simple and regular built environments (Miao et al., 2020) (Figure 2).

(2) The fisheye photography method involves taking 2D photographs of a pre-selected point in a canyon using a circular fisheye camera positioned perpendicular to the ground and aimed at the sky (Cheung et al., 2016). These photographs are processed into black-and-white images, where white areas represent open sky and black areas represent masked sky. The ratio of these areas is then calculated to obtain the SVF (L. Chen et al., 2012). Fisheye cameras can be used at various heights, such as on the ground, at car sunroof height, 1.2 meters, 1.5 meters, or 2.2 meters above ground (Matzarakis & Matuschek, 2011; Shi Bing et al., 2017). This approach was first used by Anderson to study sunlight in forest canopies and later applied to urban climatology (Anderson, 1964). Subsequent improvements by Holmer et al. (2001) introduced geometric corrections and automated photography software, saving SVF acquisition time. This method ensures high accuracy, especially for photographing tree branches and leaves, but it is labor-intensive and limited to uniformly cloudy conditions (Chapman et al., 2002)..

(3) GPS methods utilize GPS receivers to calculate SVFs by acquiring satellite visibility data (Chapman et al., 2002). These methods achieve high accuracy in urban environments with relatively sparse trees but have limited applicability in rural areas with dense tree canopies and diverse tree species (Zeng et al., 2018).

(4) The use of Street View images for data mining has emerged in recent years with the optimization and refinement of Google Street View (GSV) to represent the geometry of street canyons and estimate SVFs (Gong et al., 2019). Carrasco-Hernandez et al. (2015) proposed a freely accessible panorama generation tool, Hugin, which computes SVFs by generating fisheye images from GSV panoramas through geometric transformations (Carrasco-Hernandez et al., 2015). This approach allows for the fast acquisition of fisheye images in urban areas but requires manual stitching and merging at a later stage (X. Li et al., 2018), making it more time-consuming..

(5) 3D city-model simulation methods estimate SVF within digital urban models by combining mapping data with computational tools (L. Chen et al., 2012), and then calculate the SVF in the computer digital 3D model. This includes four common methods: 3D Sky view (Souza et al., 2004); the Solar and LongWave Environmental Irradiance Geometry model (SOLWEIG) (Lindberg et al., 2008); the Sky Helios model (Hämmerle et al., 2011; Liang et al., 2017; Fröhlich & Matzarakis, 2018) and Sky View Analysis (AntonelloDN, 2019). 3D Sky view is calculated based on the extended software of ArcView GIS version 3.2, which first represents the stereographic projection of a 3D object in coordinates, then calculates the SVF by combining the stereo network (Souza et al., 2003, 2004). This approach is advantageous for large-scale urban streets, but its accuracy is limited by the database. SOLWEIG involves creating a hemisphere with a self-contained light source at the test point of the virtual 3D model and then calculating the SVF based on the shadows. This method can be applied in complex urban environments (Lindberg et al., 2008). Munoz's method, which involves extracting raster and vector data to create a 3D site, acquiring and merging pictures from five directions: east, south, west, and north with the sky using virtual fisheye images, and then calculating the SVF (Matzarakis & Matuschek, 2011). This method is often used in microscale models (Liang et al., 2017; Fröhlich & Matzarakis, 2018). Sky View Analysis is an extension program built in SketchUp 2019 by AntonelloDN (2019). It is similar to the SVF Engine (Liang et al., 2017). First, a virtual fisheye camera is created in the 3D model in SketchUp, then a self-defined radius is used to create a hemisphere similar to the dome of the sky. Finally, a 2D SVF image is obtained on the site plane. This approach quickly obtains the SVF but may have slight errors due to the diameter of the hemisphere

Selection of the SVF Acquisition Method for This Study

Each of the SVF acquisition methods mentioned above has its own set of advantages and disadvantages, which should be chosen based on factors such as the scale of the research site, the completeness of the database, and the available hardware and software capabilities. The experimental subjects in this study comprise 210 distinct models of university-campus built environments, and multiple simulations and SVF calculations must be carried out for different date periods in need of shadow for university teachers and students. Therefore, geometric methods akin to method (1) are impractical for use in such a large database. Similarly, methods (2), (3), and (4), which rely on real-life photography, are not feasible for the virtual building models employed in this study.

Sky View Analysis in 3D city model simulation is the most suitable method to obtain SVFs for this study. First, SketchUp is widely used in architectural design practice in China, making Sky View Analysis directly compatible with existing design workflows and easier for practitioners to adopt in reference-based applications. Second, this method allows a consistent sky-dome hemisphere to be applied across multiple experimental subjects, thereby reducing workload and helping to control experimental error.

METHODOLOGY

Case Selection

Compared to mid to high latitude areas, low latitude regions, such as Guangzhou, China, which is often exposed to direct sunlight, require shading to address outdoor thermal comfort issues. Guangzhou, a mega-city located at 23.2°N latitude and 113.2°E longitude, receives substantial solar radiation (China Weather Information, 2022). The city ranks third in China in terms of the number of universities, with a total of 1.3072 million college students enrolled (China Government Network, 2022). However, the outdoor activity spaces of many universities in Guangzhou City do not provide a highly satisfactory thermal comfort environment. During the outdoor activities of teachers and students, more than 60% of the respondents reported that it was very hot or even unbearably hot (Fang et al., 2019). The shadows created by existing buildings, structures, or plants on campuses do not effectively accommodate the specific outdoor activities of teachers and students. This results in discontinuous shadows, limited shaded areas, or large sun-exposed areas within the shadows, negatively impacting outdoor activities (Luo Guohui et al., 2021; Luo Guohui, 2022).

Date Period and Time Period in Need of Shadow

SVF analysis with a fisheye camera is a useful and practical tool for any geographic location and building (Lee & Levermore, 2019). Different geographic locations have varying outdoor temperatures, solar radiation values, and different periods requiring shade for outdoor activities. Zhang et al. (2019) employed the "virtual year" method to determine the starting and ending dates of building shade demand in 10 typical cities in China, including Guangzhou (Figure 3a), based on the hourly outdoor air temperature and solar radiation data over the years (Zhang et al., 2019). Although this study focuses on indoor thermal environment demand, the outdoor shade calculation period's starting and ending dates are established through time-by-time processing of outdoor air dry-bulb temperature. This is based on raw outdoor meteorological data from 1,000 meteorological stations over 48 years and daily and monthly values from 99 meteorological stations over 30 years. These results are highly valuable for reference in this study (Figure 3b).

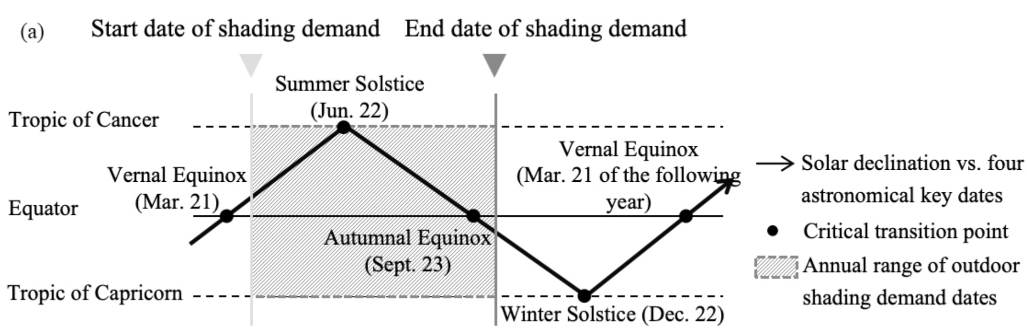

(b)

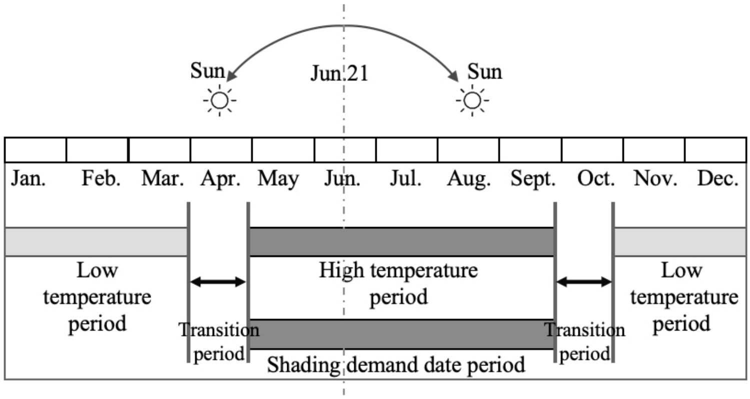

Figure 3. Variation of indoor and outdoor shading demand with changing dates (Zhang et al., 2019). (a) Start–end date range of shading demand in Guangzhou, China; (b) research on the method of determining outdoor calculation parameters for building shade design

However, unlike many full-year occupations, university teachers and students do not remain on campus throughout the entire year. Although their daily schedules and activity locations are not identical, campus use is strongly structured by the academic calendar. Therefore, the shading-demand period for campus users cannot be determined only from general urban climatic conditions, nor can it be explained only by teaching schedules. In this study, the selected dates were defined by the overlap between Guangzhou’s climatic shading-demand period and the academic-calendar-based campus activity cycle. The climatic beginning and ending dates of shading demand in Guangzhou were based on the long-term meteorological analysis by Zhang et al. (2019). Meanwhile, campus-based and Guangzhou-based thermal studies have shown that summer outdoor thermal comfort, shaded pedestrian environments, and short-term sunlight exposure during movement between academic buildings are important issues for campus users (Y. Li et al., 2024; J. Yang et al., 2025; Zhao et al., 2016). Accordingly, May 24 and October 4 were used to represent the climatic beginning and ending dates in need of shadow for Guangzhou, whereas July 15 and September 1 were used to represent academic-calendar transition dates within this climatic window. July 15 is therefore not the only applicable date, but a conservative tested condition within the campus shading-demand period; September 1 represents the return of regular campus activities while Guangzhou remains within the climatic shading-demand period.

The period between the end of the morning session and the beginning of the afternoon session is one of the most frequent attendance periods for university teachers and students, and the thermal comfort of the outdoor building environment during this period directly affects the attendance rates of teachers and students in outdoor places of higher education (Khan & Azari, 2021). Although some solar radiation is present during the morning and late afternoon hours, approximately 30–40% of the outdoor activity area remains shaded during these periods (Ghaffarianhoseini et al., 2019). In contrast, the C/A value between 12:00 and 14:00 around noon is relatively low (Figure 4), and solar radiation is often the strongest at this time of day, making it a critical period for students to perceive heat (Ma et al., 2025). Notably, the 12:00–14:00 period generally overlaps with the transition between morning classes, lunchtime, and the beginning of afternoon sessions. During this period, campus users are likely to move between teaching buildings, dining halls, offices, and dormitories, increasing their short-term exposure to direct sunlight in outdoor campus spaces (Sun et al., 2022; J. Yang et al., 2025). Consequently, the ability to construct CHS spaces that meet users' shading needs during this critical period becomes especially important (Ghaffarianhoseini et al., 2019). Therefore, the time period from 12:00 to 14:00 was chosen for simulation experiments in this study.

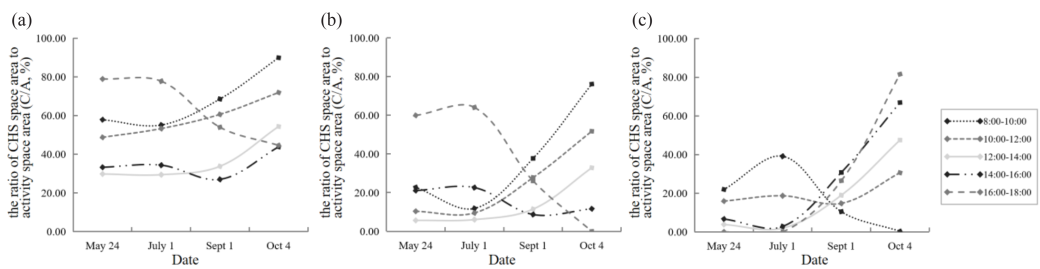

Figure 4. C/A values for the three models between 8:00 and 18:00. (a) Model 1; (b) model 2; (c) model 3

Experiment Setup

As shown in Figure 5, the experiment comprised three main methodological steps. First, SketchUp 2019 and its extension program, Sky View Analysis, were used to obtain and calculate the SVFa of each experimental subject. Second, the same SketchUp models were imported into Autodesk Ecotect Analysis for shadow simulation, as Ecotect is commonly used for sunlight and shadow analysis and can be integrated with SketchUp-based 3D modelling workflows (Amani, 2019; Lu & Du, 2013). In Ecotect, the Guangzhou geographic location, four selected experimental dates, and the 12:00–14:00 period were specified as simulation inputs. Shadow simulations were conducted at 30-minute intervals, namely 12:00, 12:30, 13:00, 13:30, and 14:00, to generate CHS-space shadow images for each experimental subject. These images were then processed to identify the effective CHS-space area within the activity space, and C/A was calculated as the ratio of CHS-space area to total activity-space area. Third, the relationship between SVFa and C/A was quantitatively analysed to obtain design-oriented reference indices for campus planning and renovation.

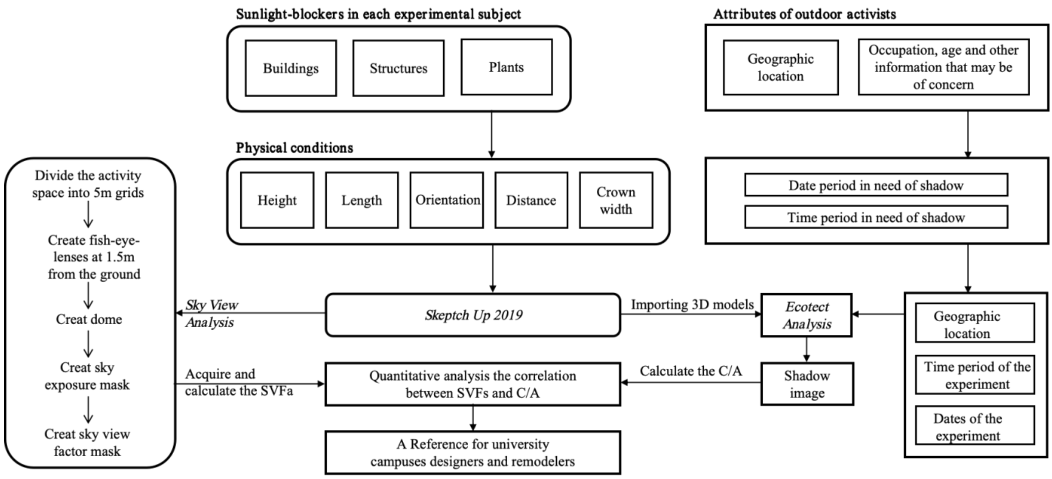

Figure 5. Methodological workflow for SVFa calculation, CHS-space shadow simulation, C/A extraction, and SVFa–C/A fitting

Because the study area is located in the Northern Hemisphere, north-south orientation has been the predominant building orientation since ancient times. In Chinese university campuses, teaching buildings and student apartments are usually six stories high because they can accommodate more functional rooms without being required to install elevators. Therefore, in this study, two north–south-oriented six-storey building blocks are selected as the base model for the experiment, and the spacing between them is set at 20 m as a representative spacing condition with reference to daylight-related planning practice in Guangzhou. Between these buildings, a hypothetical circular activity space with a 20-meter diameter was placed in the central canyon. A circular shape was chosen to minimize errors compared to square corners. There are a total of 210 such base models, each featuring different types of sunlight-blockers randomly placed in the canyons. These blockers include extended roofs, projections from buildings, ground-level sun shelves, and trees of varying heights and canopy widths. Each sunlight-blocker was arranged according to common architectural design practices while conforming to the expected scale and spacing of the experimental subjects.

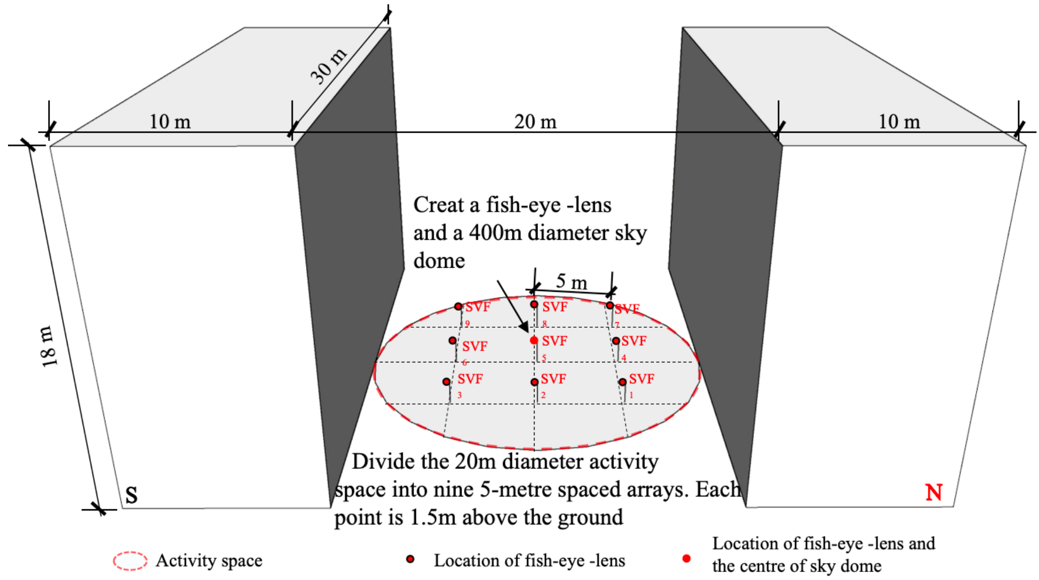

Figure 6. Division of the activity space and setup of virtual fisheye lenses and sky hemispheres

David Muñoz et al. proposed an efficient idea for calculating SVFs by dividing a large urban environment into equal-sized grid planes, and then calculating SVFs for intersections on the grid planes (Muñoz et al., 2018)such as urban physics simulations or the study of the solar impact effects at different scales, complex 3D city models are required to evaluate physical values. In this article, we propose an efficient system for quickly computing the Sky View Factor (SVF. This method can refine complex and large urban models with higher accuracy, although it increases manual time and workload. In this study, the circular event space was divided into nine point arrays with equal spacing of 5 m, and then virtual fish-eye -lenses were created with Sky View Analysis at 1.5 m pedestrian height in each point array (Shi Bing et al., 2017). Next, at the point directly above the centre of the circle, a sky dome with a diameter of 400 m was created above the centre of the circle for each experimental subject. The SVF data obtained from the 9 lattice points are labeled as “SVF1, SVF2, ..., SVF9”, and the SVFa of each experimental subject was calculated (Figure 6).

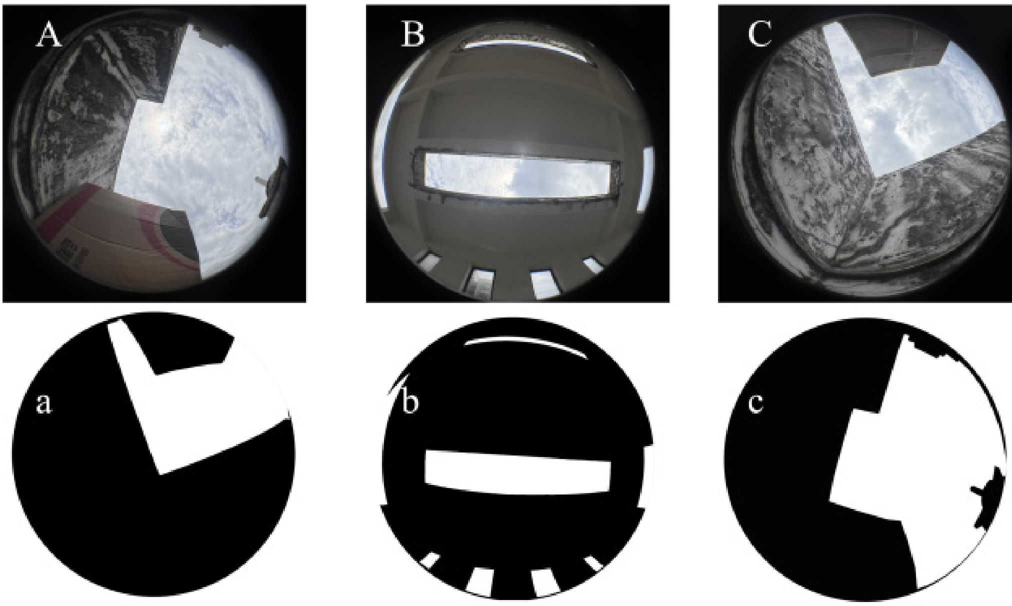

Figure 7. Field SVF photographs and corresponding measured SVF diagrams. (A, B, C) Field fisheye photographs; (a, b, c) corresponding measured SVF diagrams.

Table 1
Comparison between actual measurements and SVF values obtained using the SketchUp plug-in

No.	Measuring Height(m)	Fisheye lens photo	Fisheye lens SVF diagram	Measured SVF	SketchUp SVF	Measured SVF / SketchUp SVF
1	0.15	A	a	0.227	0.248	91.5%
2	1.5	B	b	0.190	0.210	90.5%
3	0.15	C	c	0.404	0.433	93.3%

While calculating SVFa from 9 points requires more effort compared to studies using a single fisheye camera, this method provides a broader detection range and better represents the shading conditions across the entire area (Lin et al., 2012). It also yields more objective design reference indices, minimizing errors. A 5 m spacing was adopted because the activity space is much smaller than an urban-scale study area, and this interval provides a workable balance between spatial representativeness, SVF accuracy, and modelling effort. Similarly, a 400 m sky dome was selected as a practical compromise: it is sufficiently large to approximate the real sky for campus-scale volumes, while remaining manageable for viewpoint adjustment in SketchUp and avoiding the larger errors associated with an overly small hemisphere. To verify the reliability of the Sky View Analysis plugin in SketchUp, this study conducted three SVF measurements in real-world settings using a combination of smartphones and Apexel 198° fisheye lenses—an accessible, relatively low-cost device with high accuracy (Cudney-Valenzuela et al., 2023). The measured SVF values were approximately 90–93% consistent with those obtained using the SketchUp plug-in and the selected sky-dome setting (Figure 7, Table 1), indicating that this approach provides an acceptable level of reliability for the comparative analysis in this study.

The 30-minute interval was adopted as a pragmatic compromise between temporal sensitivity and simulation workload. Previous shadow- and solar-radiation-related studies have used 30-minute intervals in sun-path division or repeated shadow computation (Takebayashi et al., 2017; Vo & Laefer, 2019). In addition, daylight and shading simulation studies have shown that hourly time steps may smooth or overlook short-term variations, whereas finer temporal resolutions are more capable of capturing transient changes (Martinho et al., 2024; Walkenhorst et al., 2002). Since this study aimed to compare 210 experimental subjects across multiple dates rather than simulate minute-level dynamic control responses, the 30-minute interval was considered sufficient to capture intra-period shadow variation while keeping simulation output, image processing, and comparative analysis manageable. The resulting CHS-space shadow images were then used to calculate the C/A ratio of each experimental subject, and the fitting relationship between SVFa and C/A was subsequently analysed across the experimental cases, as illustrated in Figure 8.

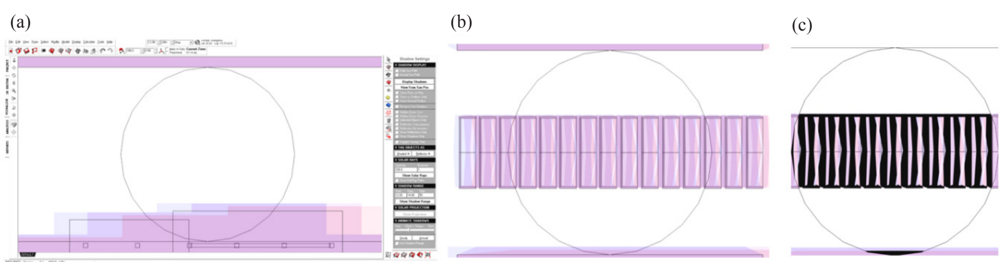

Figure 8. Ecotect simulation and image-processing workflow for CHS space identification and C/A calculation. (a) Ecotect-based simulation of CHS space during 12:00–14:00; (b) CHS space image obtained from the Ecotect simulation; (c) Processed CHS space area (black region) used for C/A calculation

RESULTS

Based on the processed ecotect simulation outputs shown in Figure 9, the CHS-space areas of the experimental subjects were extracted and converted into C/A values for further quantitative analysis. Figure 9 illustrates the workflow using one representative model as an example, and the same procedure was repeated for all 210 experimental subjects. After testing the 210 subjects, a total of 1890 SVFs were obtained, from which 210 SVFa values were calculated, corresponding to the 210 subjects. In addition, 840 C/A ratios were derived from the corresponding simulated CHS-space images. Subsequently, the relationship between SVFa and C/A was fitted through one prediction cycle, yielding the following results.

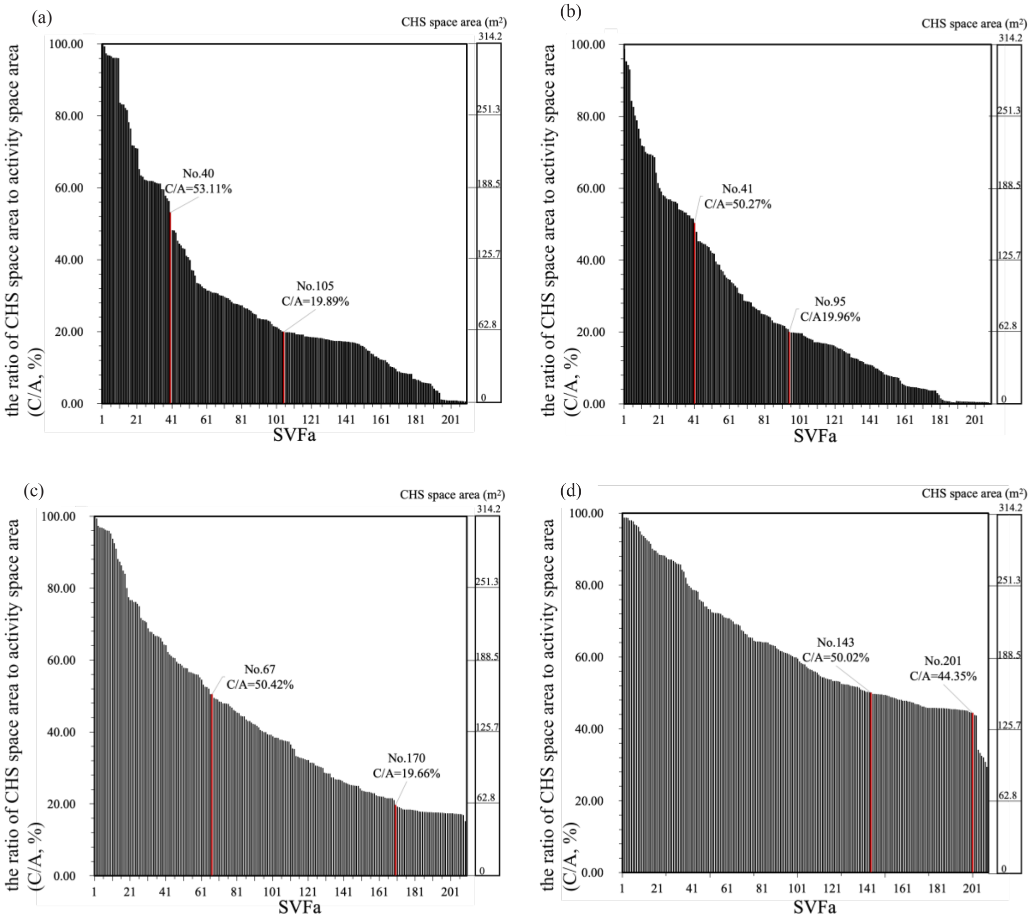

Figure 9. High-to-low distribution of C/A for different dates in need of shadow.

(a) Data distribution on May 24;(b)Data distribution on July 15;(c) Data distribution on Sept. 1;(d) Data distribution on Oct. 4

Understanding the C/A of University Campuses in Guangzhou on A Typical Date

From Figure 9, it can be seen that there is a significant difference in the C/A of different shading demand dates during the same time period. On May 24, only 40 subjects had C/A ratios exceeding 50%, which equates to 19.05% of the total 210 subjects. Conversely, as many as 106 experimental subjects had C/A ratios below 20%, accounting for 50.48% of the total. On July 15, similar trends were observed with 41 subjects (19.52%) having C/A ratios exceeding 50% and 116 subjects (55.24%) below 20%. Moving to September 1, 67 subjects (31.90%) had C/A ratios exceeding 50%, while 106 subjects (50.48%) had C/A ratios below 20%. By October 4, 143 subjects (68.10%) had C/A ratios exceeding 50%, and only one subject (0.50%) had a C/A ratio below 20%. Furthermore, SPSS analysis showed that the Cook’s distances of all experimental data were well below the conventional threshold of 1, confirming both the data integrity and the validity of randomness(Chatterjee & Hadi, 2015).

Figure 9 shows that CHS space coverage was generally limited on May 24, July 15, and September 1, compared with October 4. Although the 210 experimental subjects were generated according to common architectural design and site-layout practices, the results indicate that, without effective CHS-space construction, most outdoor activity areas remain exposed to prolonged sunlight during the shading-demand period for teachers and students. To a certain extent, this observation also aligns with the finding that over 60% of respondents among university teachers and students in Guangzhou City reported experiencing very hot or unbearably hot conditions during their outdoor activities (Fang et al., 2019).

Understanding the Fitting Relationship between SVFa and C/A in Guangzhou's University Campuses

Table 2 shows the statistical metrics for the N–S orientation on four typical dates were derived using SPSSAU (The SPSSAU Project, n.d.).

Table 2
Fitting and evaluation results of regression models for 210 N-S-oriented building configurations on 4 typical dates

Date	Fit types	R^2	Adjustment of R^2	Standard error	AIC	BIC
May 24	Quadratic Polynomial Fit	0.826	0.824	0.105	-346.262	-336.221
	Cubic Polynomial Fit	0.826	0.823	0.106	-344.262	-330.874
	Linear Fit	0.780	0.779	0.117	-299.810	-293.116
	Logarithmic Fit	0.786	0.785	0.116	-305.513	-298.819
July 15	Quadratic Polynomial Fit	0.765	0.763	0.116	-306.103	-296.062
	Cubic Polynomial Fit	0.768	0.764	0.116	-306.524	-293.136
	Linear Fit	0.740	0.739	0.121	-286.869	-280.175
	Logarithmic Fit	0.729	0.728	0.124	-278.539	-271.844
Sept. 1	Quadratic Polynomial Fit	0.793	0.791	0.106	-343.956	-333.914
	Cubic Polynomial Fit	0.795	0.792	0.106	-343.266	-329.878
	Linear Fit	0.766	0.765	0.112	-320.283	-313.589
	Logarithmic Fit	0.750	0.749	0.116	-306.315	-299.621
Oct. 4	Quadratic Polynomial Fit	0.680	0.677	0.098	-375.020	-364.978
	Cubic Polynomial Fit	0.684	0.679	0.098	-375.395	-362.007
	Linear Fit	0.659	0.658	0.101	-363.604	-356.909
	Logarithmic Fit	0.628	0.626	0.106	-345.063	-338.369

Based on simulation and testing, the quadratic polynomial consistently outperformed the cubic polynomial, linear, and logarithmic models. As shown in Table 2, it produced the lowest the Akaike Information Criterion (AIC) and the Bayesian Information Criterion (BIC) values across all four dates. The cubic polynomial performed slightly worse, while the linear and logarithmic models showed substantially poorer fit. Since the ΔAIC and

ΔBIC values compared with other models both exceeded 2 (Wagenmakers & Farrell, 2004)1973, the quadratic polynomial was confirmed as the most appropriate model, achieving the best balance between simplicity and predictive accuracy. The fitted curves are illustrated in Figure 10.

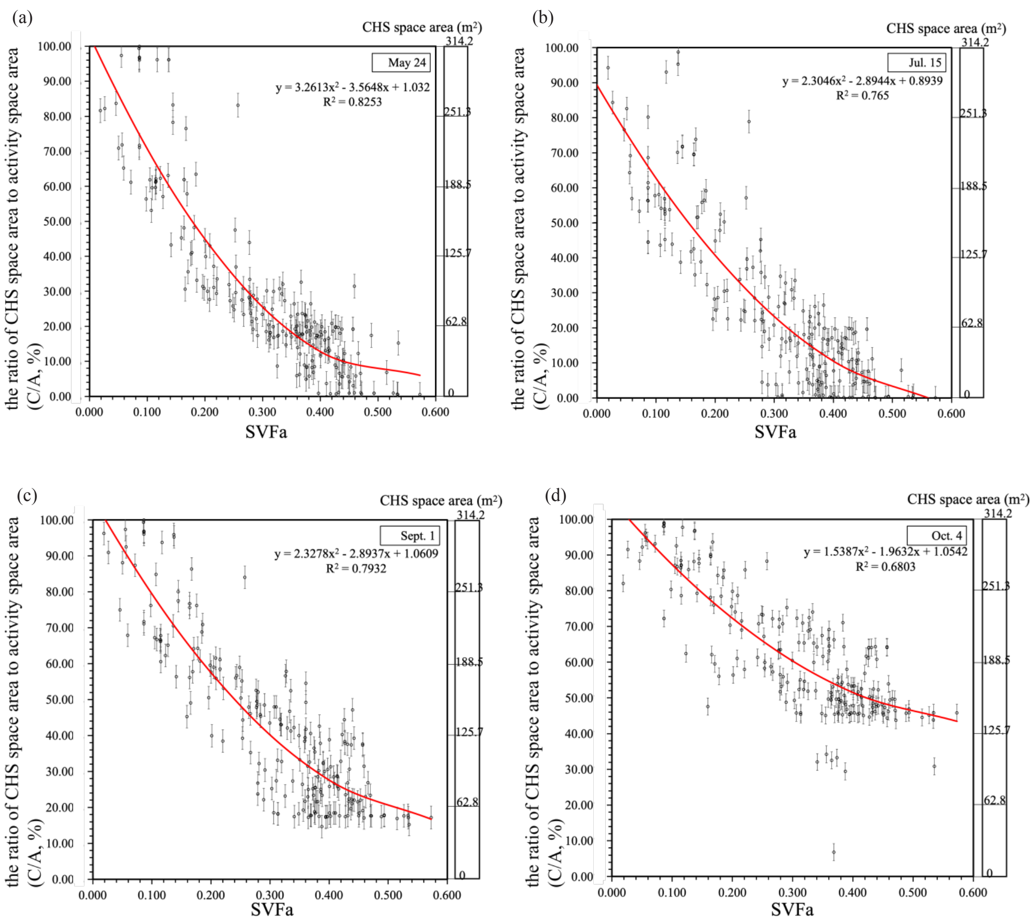

Figure 10. Fitted C/A–SVFa curves for the four typical dates

(a)Data distribution on May 24; (b)Data distribution on Jul. 15; (c) Data distribution on Sept. 1; (d) Data distribution on Oct. 4

Understanding the Relationship between SVFa-C/A on University Campuses in Guangzhou on Typical Dates

The best-fit curves for the four typical dates were combined to further compare the SVFa–C/A relationship across the tested date conditions.

Although the 210 models were classified under N–S orientations, their regression curves exhibit consistent trends, particularly in SVFa inflection zones, C/A thresholds, and slope changes. As shown in Figure 11, curves positioned closer to the horizontal axis correspond to lower C/A ratios and greater solar exposure, indicating a stronger demand for CHS space measures. A distinct transition from slow to rapid C/A growth occurs when SVFa falls to about 0.29–0.39. In design terms, this interval may be treated as a practical control band: once SVFa is reduced below about 0.39, the effectiveness of CHS-space construction improves noticeably, and the gain becomes more pronounced below about 0.29 (Table 3). Although these patterns may provide a preliminary reference for regions at similar latitudes, their application should be supported by local climatic and spatial calibration (Rao et al., 2025).

Table 3
Key changes in the SVFa–C/A fitting curves for the four typical dates

Inflection point interval		0.29–0.39
C/A at the inflection point (%) and corresponding CHS space area	May 24	0.14(25.1m^2) –0.27(53.4m^2)
	Jul. 15	0.12(25.1m^2) –0.25(53.4m^2)
	Sept. 1	0.29(72.3m^2)–0.42(103.7m^2)
	Oct. 4	0.49(157.1m^2) –0.61(179.1m^2)

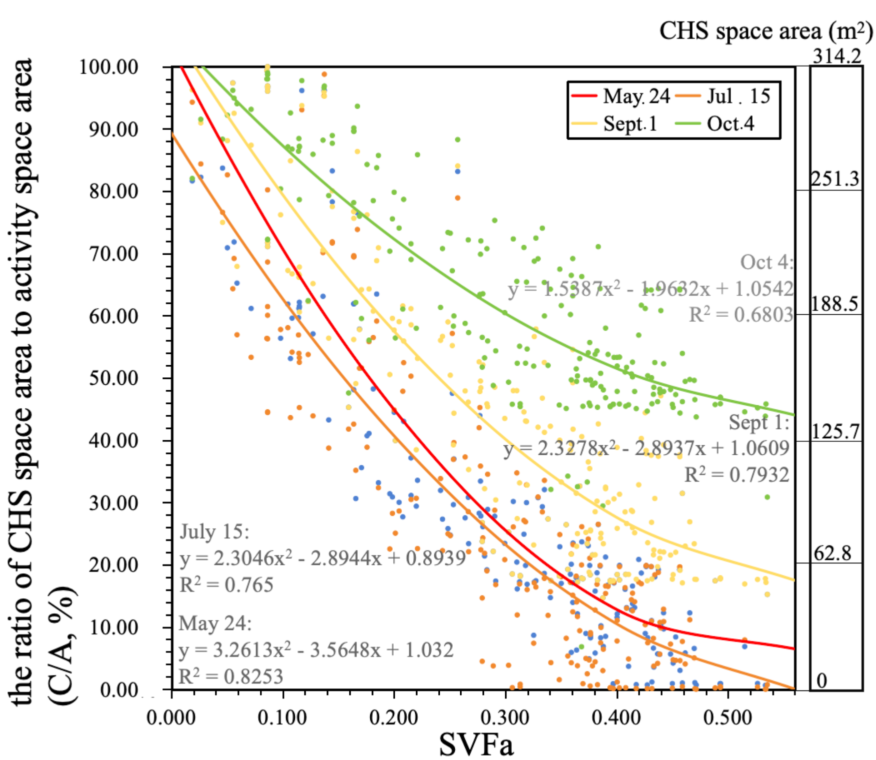

Figure 11. Combined SVFa–C/A fitting curves for the four typical dates

Regarding the correlation among the fitted curves for the four dates, Figure 11 shows that the correlation of the fitted curves for the four dates, the R^2 of the fitted curve for October 4 is the smallest, and the correlation between SVFa and C/A is the lowest. According to the calculation of solar altitude angle (Chinese Chapter of the Open Source Geospatial Foundation, 2020), the solar altitude angle in Guangzhou ranges from 49.8° to 62.6° between 12:00 and 14:00 on October 4. In contrast, on May 24, July 15, and September 1, the solar altitude angles are 62.1°-87.6°, 62.2°-88.29°, and 57.6°-75.1° respectively on these dates. Therefore, the weaker correlation observed on October 4 can likely be attributed to its lower solar altitude angle. The slanted sunlight affects the shading effectiveness differently between the dates.

Regarding the inflection points where the curves transition from gradual to rapid increases, all four fitted curves consistently show these inflection points when SVFa ranges from 0.29 to 0.39. The rate of C/A increase with decreasing SVFa is minimal across all dates from 0.56 down to 0.45, but accelerates noticeably as SVFa approaches 0 from 0.29 onwards. This suggests that when SVFa is at 0.29–0.39, the construction of CHS space enters an important turning interval regardless of the date, and the effectiveness of constructing an effective CHS space increases rapidly with the increase of sunlight-blockers inside the activity space from 0.29 onwards.

Regarding the magnitude of C/A, October 4 shows the highest values across most SVFa intervals, followed by September 1, whereas May 24 and July 15 show the lowest values. When SVFa is approximately 0.56, the baseline C/A is about 5% on May 24 and July 15, about 20% on September 1, and about 50% on October 4. This suggests that some CHS space can be formed by the building canyon itself before additional sunlight-blockers are introduced. However, the baseline C/A remains very low on May 24 and July 15, and is still limited on September 1, indicating that building massing alone cannot meet the shading needs of campus users during these dates. This finding is consistent with previous campus research showing that a considerable proportion of campus shade may be ineffective for actual outdoor use (Ghaffarianhoseini et al., 2019).

DISCUSSION

The results highlight that shade is one of the key strategies for improving urban microclimate conditions, and that outdoor shaded environments on university campuses still require greater attention from designers and researchers (Rodríguez Algeciras & Matzarakis, 2016)knowledge about the urban thermal bioclimate should be transferred into climatic guidelines for planning. The general framework of this study responds to the need of analyzing thermal bioclimate in Mediterranean climate regions and its influence as an urban design factor. The paper analyzes the background of the urban climate and thermal bioclimate conditions in Barcelona (Spain, and outdoor shaded environments on university campuses still need increased attention from relevant designers and scholars. By combining digital simulations with empirical analysis, this study identifies the SVFa inflection ranges and the associated C/A growth patterns of CHS spaces, tailored to the spatial and temporal demands of outdoor users. The results offer quantitative benchmarks for optimizing CHS space construction in high-density subtropical university campuses (Gong Zhaoxian et al., 2021). The lack of an effectively constructed CHS space makes it difficult to meet the date period, time period, and activity space in need of shadow. This study simulated and analysed 210 randomized campus-canyon configurations based on common design conventions. The results show that, among the four fitted curves, the July 15 curve produced the lowest C/A values across most SVFa intervals. Therefore, when designers are about to design or remodel a university campus in Guangzhou and regions at similar latitudes, and want to construct a CHS space of a certain scale, the July 15 curve may be used as the most conservative reference for comparable campus canyons in Guangzhou (Table 4). For example, if a CHS space with C/A≈55% is desired under the July 15 condition, the design should aim to keep SVFa at or below the corresponding threshold reported in Table 4.

Table 4
Key indicators of effective CHS space construction

Four Typical Dates		C/A						
50%		55%	60%	65%	70%	75%	80%	
SVFa	May 24	0.178	0.158	0.139	0.120	0.103	0.086	0.070
	July 15	0.155	0.133	0.111	0.091	0.071	0.052	0.033
	Sept. 1	0.240	0.213	0.188	0.164	0.141	0.119	0.098
	Oct. 4	0.422	0.356	0.304	0.258	0.217	0.180	0.146

However, it is not appropriate to blindly pursue a lower SVFa while ignoring the daylighting needs of indoor rooms, the sunlight requirements of the site, and other functional considerations. The reference values in Table 4 are not intended as universal thresholds for all dates, sites, or campus layouts. Instead, they are design-oriented benchmarks derived from four representative date conditions: May 24 and October 4 indicate the climatic beginning and ending of the shading-demand period in Guangzhou, while July 15 and September 1 correspond to key academic-calendar transitions within this climatic window. Therefore, these values are most suitable for early-stage screening and comparative assessment rather than for replacing project-specific shadow simulation. In practical campus design or renovation, designers should first define the target C/A according to activity needs, calculate the existing or proposed SVFa at pedestrian height, and compare it with the corresponding threshold in Table 4. If the calculated SVFa is higher than the target threshold, additional sun-blocking elements, such as projections, pergolas, adjustable shading devices, or vegetation with large summer crowns, can be introduced to reduce SVFa and improve CHS-space coverage. At the same time, these shading measures should be coordinated with indoor daylighting, functional circulation, site sunlight needs, maintenance, and other project-specific requirements.

CONCLUSION

This study developed a design-oriented quantitative reference for constructing CHS space in north–south university-campus canyon environments in Guangzhou. Based on 210 experimental configurations, the relationship between SVFa and C/A was fitted to clarify how built-environment openness corresponds to effective CHS-space coverage. The main contribution of this study is to translate SVFa, a geometric indicator that is relatively easy to obtain at the early design stage, into shading-performance thresholds that can support campus planning and renovation decisions.

The fitted results show a consistent transition interval across the tested dates. When SVFa decreases into approximately 0.29–0.39, C/A shifts from a relatively gradual increase to a steeper growth regime. This indicates that lowering SVFa below 0.39 generally strengthens the effectiveness of CHS space construction, with particularly pronounced improvements as SVFa approaches the lower end of the interval. For designers, this transition provides a practical target range: once SVFa enters this band, incremental additions of sun-blocking elements are more likely to yield tangible gains in effective shade coverage.

The analysis also provides conservative benchmark thresholds for early-stage campus planning and retrofit design. Among the four tested dates, July 15 represents the most unfavourable condition, under which CHS-space performance reached $C/A \geq 50\%$ at approximately $SVFa \leq 0.155$ and $C/A \geq 60\%$ at approximately $SVFa \leq 0.111$. In practical use, these thresholds can serve as a preliminary screening reference rather than fixed universal standards. Designers may first calculate the SVFa of a target activity space at pedestrian height, compare it with the threshold corresponding to the intended C/A target, and then decide whether additional sun-blocking elements are required. If the calculated SVFa is higher than the target threshold, the scheme can be adjusted through canyon geometry, projections, pergolas, vegetation, or adjustable shading devices to improve expected CHS-space coverage.

In addition, the study highlights the limits of relying solely on buildings to form functional CHS space. Under building-only configurations, effective shade coverage remains low, typically 5–20%, during the main campus shading-demand period from May 24 to September 1. This suggests that, in Guangzhou's campus environments, additional design measures beyond primary building massing are usually required to provide continuous and usable shade during the midday transition period. Potential measures include projections, pergolas, adjustable shading devices, and vegetation strategies suited to the campus context.

Overall, the findings provide a concise set of quantitative references linking SVFa to CHS-space effectiveness for dense north–south campus canyons in Guangzhou during the defined midday shading-demand period. Their transfer to other spatial types, orientations, or climatic contexts should be undertaken with local verification or calibration. Future work may broaden the applicability of the benchmarks by testing additional orientations and canyon morphologies, and by integrating SVFa-C/A thresholds with outdoor thermal-comfort indices under varying wind and radiation conditions, thereby strengthening the translation from geometric control to perceived comfort.

AUTHOR CONTRIBUTIONS STATEMENT

L. G. contributed to the conception and design of the study, methodology development, simulation setup, data analysis and interpretation, and drafting of the manuscript.

Nik Lukman Nik Ibrahim provided guidance on research framework and critically revised the manuscript for important intellectual content.

W.Z., L.J. and W.Y. contributed to data processing, model verification, and result interpretation.

C.K., G.Z., H.L., H.H., and L.W contributed to case preparation, data collection, and technical support.

All authors reviewed and approved the final version of the manuscript and agree to be accountable for all aspects of the work.

ACKNOWLEDGEMENT

This paper is part of the requirements for the first author’s doctoral degree. This research was supported by the Tabung Agihan Penyelidikan of Universiti Kebangsaan Malaysia (TAP-K013216), the Natural Science Youth Project of Guangzhou Huali College, China (HLKY-2022-ZK-01), and the 2023 Higher Education Teaching Research and Reform Project of Guangzhou Huali College. The authors thank the anonymous reviewers for their constructive comments.

DISCLOSURE STATEMENT

No potential conflict of interest was reported by the authors.

REFERENCES

Amani, N. (2019). Energy efficiency using the simulation software of atrium thermal environment in residential building: A case study. *Advances in Building Energy Research, 13*(1), 65–79. https://doi.org/10.1080/17512549.2017.1354781

Anderson, M. C. (1964). Studies of the woodland light climate: I. The photographic computation of light conditions. *Journal of Ecology, 52*(1), 27–41. https://doi.org/10.2307/2257780

AntonelloDN. (2019, August 13). *Sky View Analysis*. SketchUp Extension Warehouse. https://extensions.sketchup.com/extension/6db3286a-d4cd-4375-85ed-77110e77f7fa/0?login=true

Arnfield, A. J. (2003). Two decades of urban climate research: A review of turbulence, exchanges of energy and water, and the urban heat island. *International Journal of Climatology, 23*(1), 1–26. https://doi.org/10.1002/joc.859

Bajsanski, I., Stojakovic, V., & Jovanovic, M. (2016). Effect of tree location on mitigating parking lot insolation. *Computers, Environment and Urban Systems, 56*, 59–67. https://doi.org/10.1016/j.compenvurbsys.2015.11.006

Blennow, K. (1995). Sky view factors from high-resolution scanned fish-eye lens photographic negatives. *Journal of Atmospheric and Oceanic Technology, 12*(6), 1357–1362. https://doi.org/10.1175/1520-0426(1995)012%3C1357:SVFFHR%3E2.0.CO;2

Bourbia, F., & Boucheriba, F. (2010). Impact of street design on urban microclimate for semi-arid climate (Constantine). *Renewable Energy, 35*(2), 343–347. https://doi.org/10.1016/j.renene.2009.07.017

Bradley, A. V., Thornes, J. E., & Chapman, L. (2001). A method to assess the variation of urban canyon geometry from sky view factor transects. *Atmospheric Science Letters, 2*(1–4), 155–165. https://doi.org/10.1006/asle.2001.0039

Cameron, A. C., & Trivedi, P. K. (2005). *Microeconometrics: Methods and applications*. Cambridge University Press.

Carrasco-Hernandez, R., Smedley, A. R. D., & Webb, A. R. (2015). Using urban canyon geometries obtained from Google Street View for atmospheric studies: Potential applications in the calculation of street level total shortwave irradiances. *Energy and Buildings, 86*, 340–348. https://doi.org/10.1016/j.enbuild.2014.10.001

Chapman, L., Thornes, J., & Bradley, A. (2002). Sky-view factor approximation using GPS receivers. *International Journal of Climatology, 22*, 615–621. https://doi.org/10.1002/joc.649

Chatterjee, S., & Hadi, A. S. (2015). *Regression analysis by example*. John Wiley & Sons.

Chen, G., Rong, L., & Zhang, G. (2021). Unsteady-state CFD simulations on the impacts of urban geometry on outdoor thermal comfort within idealized building arrays. *Sustainable Cities and Society, 74*, 103187. https://doi.org/10.1016/j.scs.2021.103187

Chen, L., Ng, E., An, X., Ren, C., Lee, M., Wang, U., & He, Z. (2012). Sky view factor analysis of street canyons and its implications for daytime intra-urban air temperature differentials in high-rise, high-density urban areas of Hong Kong: A GIS-based simulation approach. *International Journal of Climatology, 32*(1), 121–136. https://doi.org/10.1002/joc.2243

Cheng, Y. (2020). *Research on the design for constant-holistically shadowed space of city leisure plaza in hot-summer area* [Master's thesis, Guangzhou University]. https://kns.cnki.net/KCMS/detail/detail.aspx?dbname=CMFD202101&filename=1020308384.nh

Cheung, H., Coles, D., & Levermore, G. (2016). Urban heat island analysis of Greater Manchester, UK using sky view factor analysis. *Building Services Engineering Research and Technology, 37*(1), 5–17. https://doi.org/10.1177/0143624415588890

Chiang, Y.-C., Liu, H.-H., Li, D., & Ho, L.-C. (2023). Quantification through deep learning of sky view factor and greenery on urban streets during hot and cool seasons. *Landscape and Urban Planning, 232*, 104679. https://doi.org/10.1016/j.landurbplan.2023.104679

China Government Network. (2022, July 3). *National list of higher education institutions*. https://www.gov.cn/xinwen/2022-07/03/content_5699066.htm

China Weather Information. (2022, November 29). *Guangzhou weather information*. http://www.weather.com.cn/cityintro/101280101.shtml

Chinese Chapter of the Open Source Geospatial Foundation. (2020, March 29). *Solar altitude angle, solar azimuth angle online calculator*. https://www.osgeo.cn/app/s1904

Cudney-Valenzuela, S. J., Arroyo-Rodríguez, V., Morante-Filho, J. C., Toledo-Aceves, T., & Andresen, E. (2023). Tropical forest loss impoverishes arboreal mammal assemblages by increasing tree canopy openness. *Ecological Applications, 33*(1), e2744. https://doi.org/10.1002/eap.2744

Du, K., Ning, J., & Yan, L. (2020). How long is the sun duration in a street canyon? Analysis of the view factors of street canyons. *Building and Environment, 172*, 106680. https://doi.org/10.1016/j.buildenv.2020.106680

Eliasson, I. (2000). The use of climate knowledge in urban planning. *Landscape and Urban Planning, 48*(1–2), 31–44. https://doi.org/10.1016/S0169-2046(00)00034-7

Emmanuel, R., Rosenlund, H., & Johansson, E. (2007). Urban shading—A design option for the tropics? A study in Colombo, Sri Lanka. *International Journal of Climatology, 27*(14), 1995–2004. https://doi.org/10.1002/joc.1609

Fang, Y. (2021). *Research on the design for systematic construction of constant-holistic shadow space in large tourist areas in hot-summer regions* [Master's thesis, Guangzhou University]. https://www.cnki.net/KCMS/detail/detail.aspx?dbcode=CMFD&dbname=CMFD202201&filename=1021633360.nh&uniplatform=OVERSEA&v=YsSBSzobS3tSnA6SVASinPf2bpLyN7MbDgVP_nUol3nOOkpQ8wZsbj6HOeBQdxbQ

Fang, Z., Xu, X., Zhou, X., Deng, S., Wu, H., Liu, J., & Lin, Z. (2019). Investigation into the thermal comfort of university students conducting outdoor training. *Building and Environment, 149*, 26–38. https://doi.org/10.1016/j.buildenv.2018.12.003

Fröhlich, D., & Matzarakis, A. (2018). Spatial estimation of thermal indices in urban areas—Basics of the SkyHelios model. *Atmosphere, 9*(6), 209. https://doi.org/10.3390/atmos9060209

Ghaffarianhoseini, A., Berardi, U., Ghaffarianhoseini, A., & Al-Obaidi, K. (2019). Analyzing the thermal comfort conditions of outdoor spaces in a university campus in Kuala Lumpur, Malaysia. *Science of the Total Environment*, *666*, 1327–1345.

Gong, F.-Y., Zeng, Z.-C., Ng, E., & Norford, L. K. (2019). Spatiotemporal patterns of street-level solar radiation estimated using Google Street View in a high-density urban environment. *Building and Environment, 148*, 547–566. https://doi.org/10.1016/j.buildenv.2018.10.025

Gong, F.-Y., Zeng, Z.-C., Zhang, F., Li, X., Ng, E., & Norford, L. K. (2018). Mapping sky, tree, and building view factors of street canyons in a high-density urban environment. *Building and Environment*, *134*, 155–167.

Gong, Z., Lu, J., & Li, Y. (2021). The spatiotemporal analysis system in the design for constant-holistic shadow space in hot summer area. *Journal of Guangzhou University (Natural Science Edition), 20*(4).

Grimmond, C. S. B., Potter, S. K., Zutter, H. N., & Souch, C. (2001). Rapid methods to estimate sky-view factors applied to urban areas. *International Journal of Climatology, 21*(7), 903–913. https://doi.org/10.1002/joc.659

Hämmerle, M., Gál, T., Unger, J., & Matzarakis, A. (2011). Comparison of models calculating the sky view factor used for urban climate investigations. *Theoretical and Applied Climatology, 105*(3), 521–527. https://doi.org/10.1007/s00704-011-0402-3

He, X., Miao, S., Shen, S., Li, J., Zhang, B., Zhang, Z., & Chen, X. (2015). Influence of sky view factor on outdoor thermal environment and physiological equivalent temperature. *International Journal of Biometeorology, 59*(3), 285–297. https://doi.org/10.1007/s00484-014-0841-5

Holmer, B., Postgård, U., & Eriksson, M. (2001). Sky view factors in forest canopies calculated with IDRISI. *Theoretical and Applied Climatology, 68*(1), 33–40. https://doi.org/10.1007/s007040170051

Hsieh, C.-M., Jan, F.-C., & Zhang, L. (2016). A simplified assessment of how tree allocation, wind environment, and shading affect human comfort. *Urban Forestry & Urban Greening*, *18*, 126–137.

Huang, Z., Cheng, B., Gou, Z., & Zhang, F. (2019). Outdoor thermal comfort and adaptive behaviors in a university campus in China's hot summer–cold winter climate region. *Building and Environment, 165*, 106414. https://doi.org/10.1016/j.buildenv.2019.106414

Jamei, E., Rajagopalan, P., Seyedmahmoudian, M., & Jamei, Y. (2016). Review on the impact of urban geometry and pedestrian level greening on outdoor thermal comfort. *Renewable and Sustainable Energy Reviews, 54*, 1002–1017. https://doi.org/10.1016/j.rser.2015.10.104

Johnson, G. T., & Watson, I. D. (1984). The determination of view-factors in urban canyons. *Journal of Applied Meteorology and Climatology*, *23*(2), 329–335.

Khan, Z., & Azari, R. (2021). Outdoor thermal comfort and human behavior: Factors, models, and methodologies. In R. Azari & H. Rashed-Ali (Eds.), *Research methods in building science and technology* (pp. 131–149). Springer. https://doi.org/10.1007/978-3-030-73692-7_7

Kim, H., & Yi, Y. K. (2019). QuVue implementation for decisions related to high-rise residential building layouts. *Building and Environment, 148*, 116–127. https://doi.org/10.1016/j.buildenv.2018.10.055

Lam, C. K. C., Shooshtarian, S., & Kenawy, I. (2023). Assessment of urban physical features on summer thermal perceptions using the local climate zone classification. *Building and Environment, 236*, 110265. https://doi.org/10.1016/j.buildenv.2023.110265

Lau, S. S. Y., Zhang, J., & Tao, Y. (2019). A comparative study of thermal comfort in learning spaces using three different ventilation strategies on a tropical university campus. *Building and Environment*, *148*, 579–599.

Lee, K., & Levermore, G. J. (2019). Sky view factor and sunshine factor of urban geometry for urban heat island and renewable energy. *Architectural Science Review, 62*(1), 26–34. https://doi.org/10.1080/00038628.2018.1536601

Li, X., Ratti, C., & Seiferling, I. (2018). Quantifying the shade provision of street trees in urban landscape: A case study in Boston, USA, using Google Street View. *Landscape and Urban Planning, 169*, 81–91. https://doi.org/10.1016/j.landurbplan.2017.08.011

Li, Y., Zhai, Z., Tian, Y., Fang, Z., Jiang, X., Mao, Y., & Zheng, Y. (2024). Differences in human thermal and physiological responses under corridor and greenway in summer in Guangzhou. *Case Studies in Thermal Engineering, 61*, 105049. https://doi.org/10.1016/j.csite.2024.105049

Liang, J., Gong, J., Sun, J., & Liu, J. (2017). A customizable framework for computing sky view factor from large-scale 3D city models. *Energy and Buildings, 149*, 38–44. https://doi.org/10.1016/j.enbuild.2017.05.024

Lin, T.-P., Matzarakis, A., & Hwang, R.-L. (2010). Shading effect on long-term outdoor thermal comfort. *Building and Environment, 45*(1), 213–221. https://doi.org/10.1016/j.buildenv.2009.06.002

Lin, T.-P., Tsai, K.-T., Hwang, R.-L., & Matzarakis, A. (2012). Quantification of the effect of thermal indices and sky view factor on park attendance. *Landscape and Urban Planning*, *107*(2), 137–146.

Lindberg, F., Holmer, B., & Thorsson, S. (2008). SOLWEIG 1.0—Modelling spatial variations of 3D radiant fluxes and mean radiant temperature in complex urban settings. *International Journal of Biometeorology, 52*(7), 697–713. https://doi.org/10.1007/s00484-008-0162-7

Lu, M., & Du, J. (2013). Assessing the daylight and sunlight availability in high-density residential areas: A case in North-East China. *Architectural Science Review, 56*(2), 168–182. https://doi.org/10.1080/00038628.2012.729311

Lu, X. (2020). *Research on the design method of outdoor "constant-holistically shadowed" space in the medical building of hot-summer area* [Master's thesis, Guangzhou University]. https://kns.cnki.net/KCMS/detail/detail.aspx?dbname=CMFD202101&filename=1020308368.nh

Luo, G., Ibrahim, N. L. N., Kaiyi, C., Gong, Z., Lijun, H., Huang, H., Wang, Z., & Luo, W. (2025). Constructing "Constant-holistical Shadow" Space for Universities in Guangzhou under the Various Roads Orientation. *Jurnal Kejuruteraan*. https://api.semanticscholar.org/CorpusID:278990815

Luo, G. (2022). *Research on the design method of complementary shadows of outdoor "constant-holistical shadow" space in hot-summer area* [Master's thesis, Guangzhou University].

Luo, G., Gong, Z., Liu, Y., & Li, Y. (2021). The deficiency of "constant-holistic shadow" space and its supplemental mechanism in hot-summer area. *Urbanism and Architecture, 18*(34), 61–65. https://doi.org/10.19892/j.cnki.csjz.2021.34.14

Ma, X., Zhang, Z., Chen, Y., & Zhang, W. (2025). How campus green space elements differently influence students' thermal perception during transition seasons? *International Journal of Thermal Sciences, 212*, 109767. https://doi.org/10.1016/j.ijthermalsci.2025.109767

Mahmoud, H., & Ragab, A. (2020). Urban geometry optimization to mitigate climate change: Towards energy-efficient buildings. *Sustainability, 13*(1), 27. https://doi.org/10.3390/su13010027

Mahmoud, R. M. A., & Abdallah, A. S. H. (2022). Assessment of outdoor shading strategies to improve outdoor thermal comfort in school courtyards in hot and arid climates. *Sustainable Cities and Society, 86*, 104147. https://doi.org/10.1016/j.scs.2022.104147

Martinho, H., Loonen, R., & Hensen, J. (2024). Evaluating the impact of high-resolution irradiation data on the daylight performance assessment of adaptive solar shading systems. *Building and Environment, 262*, 111816. https://doi.org/10.1016/j.buildenv.2024.111816

Matzarakis, A., & Matuschek, O. (2011). Sky view factor as a parameter in applied climatology: Rapid estimation by the SkyHelios model. *Meteorologische Zeitschrift, 20*(1), 39–45. https://doi.org/10.1127/0941-2948/2011/0499

Miao, C., Yu, S., Hu, Y., Zhang, H., He, X., & Chen, W. (2020). Review of methods used to estimate the sky view factor in urban street canyons. *Building and Environment, 168*, 106497. https://doi.org/10.1016/j.buildenv.2019.106497

Morakinyo, T. E., Dahanayake, K. K. C., Adegun, O. B., & Balogun, A. A. (2016). Modelling the effect of tree shading on summer indoor and outdoor thermal condition of two similar buildings in a Nigerian university. *Energy and Buildings, 130*, 721–732. https://doi.org/10.1016/j.enbuild.2016.08.087

Muñoz, D., Beckers, B., Besuievsky, G., & Patow, G. (2018). A technique for massive sky view factor calculations in large cities. *International Journal of Remote Sensing, 39*(12), 4040–4058. https://doi.org/10.1080/01431161.2018.1452071

Nikolopoulou, M., Baker, N., & Steemers, K. (2001). Thermal comfort in outdoor urban spaces: Understanding the human parameter. *Solar Energy, 70*(3), 227–235. https://doi.org/10.1016/S0038-092X(00)00093-1

Nikolopoulou, M., & Steemers, K. (2003). Thermal comfort and psychological adaptation as a guide for designing urban spaces. *Energy and Buildings, 35*(1), 95–101. https://doi.org/10.1016/S0378-7788(02)00084-1

Niu, J., Hong, B., Geng, Y., Mi, J., & He, J. (2020). Summertime physiological and thermal responses among activity levels in campus outdoor spaces in a humid subtropical city. *Science of the Total Environment, 728*, 138757. https://doi.org/10.1016/j.scitotenv.2020.138757

Oke, T. R. (1981). Canyon geometry and the nocturnal urban heat island: Comparison of scale model and field observations. *Journal of Climatology, 1*(3), 237–254. https://doi.org/10.1002/joc.3370010304

Palme, M., Privitera, R., & La Rosa, D. (2020). The shading effects of green infrastructure in private residential areas: Building performance simulation to support urban planning. *Energy and Buildings, 229*, 110531. https://doi.org/10.1016/j.enbuild.2020.110531

Peng, F., Wong, M. S., Ho, H. C., Nichol, J., & Chan, P. W. (2017). Reconstruction of historical datasets for analyzing spatiotemporal influence of built environment on urban microclimates across a compact city. *Building and Environment*, *123*, 649–660.

Peng, F., Xiong, Y., & Zou, B. (2021). Identifying the optimal travel path based on shading effect at pedestrian level in cool and hot climates. *Urban Climate, 40*, 100988. https://doi.org/10.1016/j.uclim.2021.100988

Rao, P., Torreggiani, D., Tassinari, P., Rötzer, T., Pauleit, S., & Rahman, M. A. (2025). Do urban green spaces cool cities differently across latitudes? Spatial variability and climatic drivers of vegetation-induced cooling. *Sustainable Cities and Society, 130*, 106513. https://doi.org/10.1016/j.scs.2025.106513

Rodríguez Algeciras, J. A., & Matzarakis, A. (2016). Quantification of thermal bioclimate for the management of urban design in Mediterranean climate of Barcelona, Spain. *International Journal of Biometeorology, 60*(8), 1261–1270. https://doi.org/10.1007/s00484-015-1121-8

Saneinejad, S., Moonen, P., & Carmeliet, J. (2014). Comparative assessment of various heat island mitigation measures. *Building and Environment, 73*, 162–170. https://doi.org/10.1016/j.buildenv.2013.12.013

Shi, B., Wang, X., & Zhao, D. (2017). Numerical simulation of the effects of sky-view factor on thermal environment in urban residential districts. *Chinese Journal of Applied Mechanics, 34*(6), 1181–1186.

Shih, W.-M., Lin, T.-P., Tan, N.-X., & Liu, M.-H. (2017). Long-term perceptions of outdoor thermal environments in an elementary school in a hot-humid climate. *International Journal of Biometeorology, 61*(9), 1657–1666. https://doi.org/10.1007/s00484-017-1345-x

Souza, L. C. L., Pedrotti, F. S., & Leme, F. T. (2004). *Urban geometry and electrical energy consumption in a tropical city*. http://hdl.handle.net/11449/230987

Souza, L. C. L., Rodrigues, D. S., & Mendes, J. F. G. (2003). The 3D Sky View extension: An urban geometry access tool in a geographical information system. In *Proceedings of the Fifth International Conference on Urban Climate* (Vol. 2, pp. 413–416).

Steyn, D. G. (1980). The calculation of view factors from fisheye-lens photographs: Research note. *Atmosphere-Ocean, 18*(3), 254–258. https://doi.org/10.1080/07055900.1980.9649091

Sun, Y., Luo, X., & Ming, H. (2022). Analyzing the time-varying thermal perception of students in classrooms and its influencing factors from a case study in Xi’an, China. *Buildings, 12*(1), 75. https://doi.org/10.3390/buildings12010075

Svensson, M. K., & Eliasson, I. (2002). Diurnal air temperatures in built-up areas in relation to urban planning. *Landscape and Urban Planning*, *61*(1), 37–54. https://doi.org/10.1016/S0169-2046(02)00076-2

Takebayashi, H., Kasahara, M., Tanabe, S., & Kouyama, M. (2017). Analysis of solar radiation shading effects by trees in the open space around buildings. *Sustainability, 9*(8), 1398. https://doi.org/10.3390/su9081398

Taleghani, M. (2018). The impact of increasing urban surface albedo on outdoor summer thermal comfort within a university campus. *Urban Climate*, *24*, 175–184.

The SPSSAU Project. (n.d.). SPSSAU (Version 25.0). Retrieved July 9, 2025, from https://spssau.com/

Unger, J. (2009). Connection between urban heat island and sky view factor approximated by a software tool on a 3D urban database. *International Journal of Environment and Pollution, 36*(1–3), 59–80. https://doi.org/10.1504/IJEP.2009.021817

Vo, A. V., & Laefer, D. F. (2019). A big data approach for comprehensive urban shadow analysis from airborne laser scanning point clouds. *ISPRS Annals of the Photogrammetry, Remote Sensing and Spatial Information Sciences, IV-4/W8*, 131–137. https://doi.org/10.5194/isprs-annals-IV-4-W8-131-2019

Wagenmakers, E.-J., & Farrell, S. (2004). AIC model selection using Akaike weights. *Psychonomic Bulletin & Review*, *11*(1), 192–196. https://doi.org/10.3758/BF03206482

Walkenhorst, O., Luther, J., Reinhart, C., & Timmer, J. (2002). Dynamic annual daylight simulations based on one-hour and one-minute means of irradiance data. *Solar Energy*, *72*(5), 385–395.

Watson, I. D., & Johnson, G. T. (1987). Graphical estimation of sky view-factors in urban environments. *Journal of Climatology, 7*(2), 193–197. https://doi.org/10.1002/joc.3370070210

Wei, R., Song, D., Wong, N. H., & Martin, M. (2016). Impact of urban morphology parameters on microclimate. *Procedia Engineering, 169*, 142–149. https://doi.org/10.1016/j.proeng.2016.10.017

Wong, N. H., & Yu, C. (2005). Study of green areas and urban heat island in a tropical city. *Habitat International, 29*(3), 547–558. https://doi.org/10.1016/j.habitatint.2004.04.008

Yang, J., Li, H., Fang, Z., Li, Y., Lu, F., Guo, T., Zhang, X., Lin, C., & Lu, J. (2025). Study on thermal and physiological responses during summer while moving between academic buildings under different walking conditions. *Case Studies in Thermal Engineering, 66*, 105809. https://doi.org/10.1016/j.csite.2025.105809

Yang, W., Wong, N. H., & Jusuf, S. K. (2013). Thermal comfort in outdoor urban spaces in Singapore. *Building and Environment, 59*, 426–435. https://doi.org/10.1016/j.buildenv.2012.09.008

Yang, Y., Zhou, D., Gao, W., Zhang, Z., Chen, W., & Peng, W. (2018). Simulation on the impacts of the street tree pattern on built summer thermal comfort in cold region of China. *Sustainable Cities and Society*, *37*, 563–580.

Zeng, L., Lu, J., Li, W., & Li, Y. (2018). A fast approach for large-scale sky view factor estimation using street view images. *Building and Environment, 135*, 74–84. https://doi.org/10.1016/j.buildenv.2018.03.009

Zhang, X., Liu, Y., Yang, L., Liu, T., Zhang, C., & Dong, H. (2019). Research on the determination method of outdoor design conditions of sun shading design. *Building Science, 35*(Issue), 98–106.

Zhao, L., Zhou, X., Li, L., He, S., & Chen, R. (2016). Study on outdoor thermal comfort on a campus in a subtropical urban area in summer. *Sustainable Cities and Society*, *22*, 164–170.

Zhou, H., Wang, X., Li, Y., Han, F., & Hu, D. (2016). Horizontal heat flux between urban buildings and soil and its influencing factors. *Sains Malaysiana*, *45*(5), 689–697.